# Nanoplasmonic couplers and splitters

**Rami A. Wahsheh, Zhaolin Lu * and Mustafa A. G. Abushagur**

*Microsystems Engineering, Kate Gleason College of Engineering,*
*Rochester Institute of Technology, Rochester, New York 14623, USA*
**zxleen@rit.ed*

**Abstract:** In this paper, we present novel designs and analysis of ultra-compact couplers and 1 × 2 splitters based on plasmonic waveguides. Numerical simulation shows coupling efficiency up to 88% for the former one and 45% for each branch for the latter one. The proposed coupler design has the advantages of improving the alignment tolerance of the plasmonic waveguide with respect to the dielectric waveguide and broadening the spectrum response of the splitter.



**OCIS codes:** (130.3120) Integrated optics devices; (230.7370) Waveguides; (240.6680) Surface plasmons.

## References and links

1. W. L. Barnes, A. Dereux, and T. W. Ebbesen, "Surface plasmon subwavelength optics," Nature **424**(6950), 824–830 (2003).
2. R. Zia, M. D. Selker, P. B. Catrysse, and M. L. Brongersma, "Geometries and materials for subwavelength surface plasmon modes," J. Opt. Soc. Am. **21**(12), 2442–2446 (2004).
3. E. N. Economou, "Surface plasmons in thin films," Phys. Rev. **182**(2), 539–554 (1969).
4. D. F. P. Pile, T. Ogawa, D. K. Gramotnev, Y. Matsuzaki, K. C. Vernon, K. Yamaguchi, T. Okamoto, M. Haraguchi, and M. Fukui, "Two-dimensionally localized modes of a nanoscale gap plasmon waveguide," Appl. Phys. Lett. **87**(26), 261114 (2005).
5. R. Coccioli, M. Boroditsky, K. W. Kim, Y. Rahmat-Samii, and E. Yablonovitch, "Smallest possible electromagnetic mode volume in a dielectric cavity," IEE Proc., Optoelectron. **145**(6), 391–397 (1998).
6. G. Veronis, and S. Fan, "Theoretical investigation of compact couplers between dielectric slab waveguides and two-dimensional metal-dielectric-metal plasmonic waveguides," Opt. Express **15**(3), 1211–1221 (2007).
7. P. Ginzburg, and M. Orenstein, "Plasmonic transmission lines: from micro to nano scale with λ/4 impedance matching," Opt. Express **15**(11), 6762–6767 (2007).
8. D. F. P. Pile, and D. K. Gramotnev, "Adiabatic and nonadiabatic nanofocusing of plasmons by tapered gap plasmon waveguides," Appl. Phys. Lett. **89**(4), 041111 (2006).
9. P. Ginzburg, D. Arbel, and M. Orenstein, "Gap plasmon polariton structure for very efficient microscale-to-nanoscale interfacing," Opt. Express **31**, 3288–3290 (2006).
10. R. Charbonneau, N. Lahoud, G. Mattiussi, and P. Berini, "Demonstration of integrated optics elements based on long-ranging surface plasmon polaritons," Opt. Express **13**(3), 977–984 (2005).
11. R. Charbonneau, C. Scales, I. Breukelaar, S. Fafard, N. Lahoud, G. Mattiussi, and P. Berini, "Passive integrated optics elements based on long-range surface plasmon polaritons," J. Lightwave Technol. **24**(1), 477–494 (2006).
12. C. Manolatou, S. G. Johnson, S. Fan, P. R. Villeneuve, H. A. Haus, and J. D. Joannopoulos, "High-density integrated optics," J. Lightwave Technol. **17**(9), 1682–1692 (1999).
13. J. S. Jensen, and O. Sigmund, "Topology optimization of photonic crystal structures: A high-bandwidth low-loss T-junction waveguide," J. Opt. Soc. Am. B **22**(6), 1191–1198 (2005).
14. G. Veronis, and S. Fan, "Bends and splitters in metal-dielectric-metal subwavelength plasmonic waveguides," Appl. Phys. Lett. **87**(13), 131102 (2005).
15. B. Wang, and G. P. Wang, "Surface Plasmon polariton propagation in nanoscale metal gap waveguides," Opt. Express **29**, 1992–1994 (2004).
16. Z. Han, L. Liu, and E. Forsberg, "Ultra-compact directional couplers and Mach-Zehnder interferometers employing surface Plasmon polaritons," Opt. Commun. **259**(2), 690–695 (2006).
17. R. A. Wahsheh, Z. Lu, and M. A. G. Abushagur, "Nanoplasmonic Directional Couplers and Mach-Zehnder Inerferometers," Opt. Commun. (to be published).
18. A. Taflove, *Computational Electrodynamics* (Artech, Norwood, MA, 1995).
19. J. P. Berenger, "A perfectly matched layer for the absorption for electromagnetic waves," J. Comput. Phys. **114**(2), 185–200 (1994).
20. R. A. Wahsheh, Z. Lu, and M. A. G. Abushagur, "Efficient couplers and splitters from dielectric waveguides to plasmonic waveguides", in Frontiers in Optics, OSA Technical Digest (CD) (Optical Society of America, 2008), paper FThS4. *http://www.opticsinfobase.org/abstract.cfm?URI=FiO-2008-FThS4*

#114470 - $15.00 USD Received 21 Jul 2009; revised 14 Sep 2009; accepted 22 Sep 2009; published 7 Oct 2009

## 1. Introduction

Recent interest arises in plasmonic waveguides (i.e., waveguides in conjunction with surface plasmons), which promise to play an important role in minimizing the footprint required to integrate multiple optoelectronic devices on the same chip. In particular, plasmonic waveguides formed by metal-dielectric-metal (MDM) structures can tightly confine light in the dielectric region on deep sub-wavelength scales [1–4] which is not possible using conventional dielectric waveguides due to diffraction limit [5]. However, the smaller the modal size in the dielectric region of the MDM, the larger the propagation loss due to the metallic losses. The tradeoff between mode confinement and propagation loss can be addressed by integrating both dielectric waveguides and plasmonic waveguides in the same system. To this end, efficient coupling between dielectric waveguides and plasmonic waveguides is of great significance.

It is necessary to use dielectric waveguides to connect the plasmonic devices to the light source and detector so that the propagation losses due to the metallic interaction are dramatically reduced. To achieve that, several different coupling methods have been proposed to increase the coupling efficiency from a dielectric waveguide into a plasmonic waveguide, such as direct coupling [6], multi-section taper [6], λ/4 coupler [7], adiabatic tapered coupler [8], and nonadiabatic tapered coupler [8,9]. Also, several different T- and Y-shaped splitters have been proposed [10–14]. Splitters are used in optical circuit elements and devices such as Mach-Zehnder interferometers (MZIs) [15–17] because they are considered as the platform for the optical sensors. In Y-junctions, the radius of curvature plays an important role in reducing radiation losses and increasing the size of the fabricated devices [10,11]. In T-junctions, the intersection area should be designed to increase the coupling efficiency and reduce back reflection. Coupling efficiency can be increased using a resonant cavity at the intersection area [12], using photonic crystal waveguides [13], or using plasmonic waveguides [14].

A recent numerical simulation demonstrated a coupling efficiency of 68% by directly coupling light from a 300 nm wide silicon waveguide into a 40 nm silver-air-silver plasmonic waveguide [6]. Coupling efficiency was further improved to 93% by using a multi-section taper of a length of 400 nm, which was designed by a genetic global optimization algorithm and analyzed with a finite-difference frequency-domain methodology. In this work, we propose a direct yet efficient short plasmonic coupler of a length of 33 nm to increase the coupling efficiency between a silicon waveguide and a silver-air-silver plasmonic waveguide. Based on the coupler, we also propose a splitter that delivers light from a silicon waveguide into two plasmonic waveguides. To the best of our knowledge, this is the first time that one reports a 1 × 2 splitter from a silicon waveguide into two MDM plasmonic waveguides. The coupling efficiency and the spectrum response of both devices are investigated using the two-dimensional (2D) finite-difference time-domain method [18] with a uniform mesh size of 1 nm to accurately capture the change of the field at the interface between the dielectric and plasmonic waveguides. The fundamental transverse magnetic mode is excited in the single-mode dielectric waveguide and the transmitted power is measured by a power monitor that is placed close to the interface with the single-mode plasmonic waveguide [6]. Then, the coupling efficiency is calculated by normalizing the transmitted power with respect to the input power. The perfectly matched layer is used to attenuate the field within its region without back reflection [19]. The metal losses are included in our simulations and the relative permittivity of the silver at the free-space wavelength $\lambda_o$ = 1.55 μm using the commercial software FullWAVE from RSOFT is −103.7 + 8.1j.

In order to validate our results, we started by simulating the structure proposed by Veronis and Fan [6] and obtained the same coupling efficiency (68%) by directly coupling light from a 300 nm wide silicon waveguide into a 40 nm silver-air-silver plasmonic waveguide. By analyzing the numerical results, it is obvious that the light wave from the dielectric waveguide

#114470 - $15.00 USD Received 21 Jul 2009; revised 14 Sep 2009; accepted 22 Sep 2009; published 7 Oct 2009

excites surface plasmon polaritons (SPPs) along the dielectric-plasmonic boundaries and the SPPs will be "funneled" into the MDM plasmonic waveguides. This funneling process can conceptually explain why light can be efficiently coupled from a large (300 nm) dielectric waveguide into a tiny (40 nm) dielectric slot MDM waveguide. Recently, we found that the coupling efficiency can be greatly improved simply by incorporating a rectangular air-gap (i.e., slot waveguide) and hence preventing transverse "funneling leakage" at the interface between the dielectric waveguide and the MDM plasmonic waveguide [20]. Herein, we present the design steps and numerical results for the proposed air-gap couplers (AGCs) and splitters.

## 2. Air-gap coupler design

First, we consider an ultra-short matching rectangular AGC inside the plasmonic waveguide at the interface with silicon, as shown in Fig. 1(a). In the 2D simulation, we varied the dimensions of the coupler and measured the corresponding coupling efficiency. The dependence of the coupling efficiency on the coupler's width $W$ and length $L$ is shown in Fig. 1(b). We found that coupling efficiency had a maximum value when $W$ matches the width of the silicon waveguide. In particular, the coupling efficiency is above 87.7% for 30 nm < $L$ < 40 nm and is maximized for $L$ = 33 nm (coupling efficiency = 88.1%). Tapering the edges of the rectangular AGC can further increase the coupling efficiency to 90% [20], but doing so will also increase the fabrication complexity. In this work, we only consider the rectangular AGC and optimize its length as 40 nm to match that of the width of the plasmonic waveguide. The field distribution of the coupled light for the rectangular AGC is shown in Fig. 1(c).

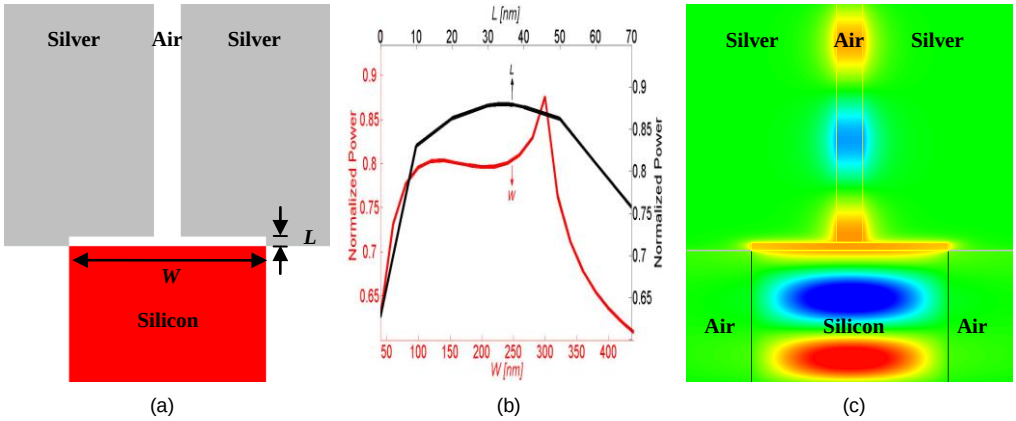


Fig. 1. (a) Schematic of the basic proposed coupler (top view). (b) Coupling efficiency as a function of the coupler's width $W$ and length $L$. (c) Field distribution of the coupled light at $\lambda_o$ = 1.55 μm for the air-gap coupler.

Veronis and Fan [6] found that to maximize the coupling efficiency between the dielectric waveguide and the plasmonic waveguide, there is an optimal width of the dielectric waveguide for a given width of the plasmonic waveguide. As shown in Fig. 2, the optimal width of the dielectric waveguide is 300 nm when the width of the plasmonic waveguide is 40 nm. We found that this dependency is broadened when using our proposed AGC. Increasing the size of the dielectric waveguide from 300 nm to 500 nm resulted in a decrease in the coupling efficiency by about 15% as opposed to 45% for the case without using the AGC.

#114470 - $15.00 USD Received 21 Jul 2009; revised 14 Sep 2009; accepted 22 Sep 2009; published 7 Oct 2009

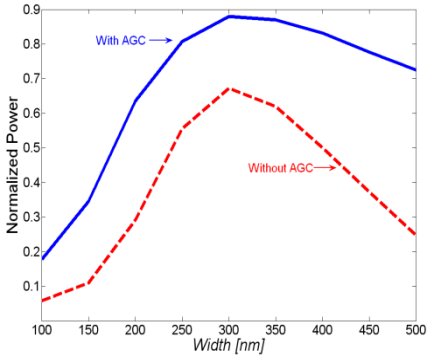


Fig. 2. Coupling efficiency for the basic structure [Fig. 1(c)] as a function of the dielectric waveguide's width.

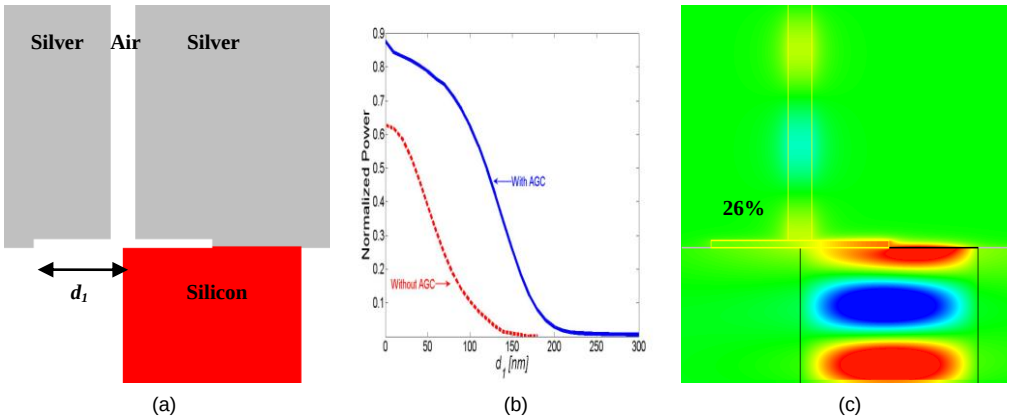


Fig. 3. (a) Schematic of the position misalignment $d_1$ between the silicon waveguide and the plasmonic waveguide with the AGC connected to it. (b) Coupling efficiency as a function of $d_1$. (c) Field distribution for the structure shown in Fig. 3(a) when $d_1$ = 150 nm.

Moreover, our coupler allows for considerable alignment tolerance, which is necessary for practical applications since accurately aligning the silicon waveguide to the plasmonic waveguide is a difficult task. To evaluate the effect of the misalignment, two configurations are examined. One is for the misalignment of both the MDM waveguide and the AGC with respect to the silicon waveguide as a function of the displacement $d_1$ [as shown in Fig. 3(a)]. Another is for the misalignment of the MDM waveguide with respect to both AGC and silicon waveguide as a function of the displacement $d_2$ [as shown in Fig. 4(a)]. The misalignment in both cases is exaggerated in order to show the effect of using the AGC. Figures 3(b) and 4(b) show the coupling efficiency with and without using the AGC as a function of the displacement $d_1$ and $d_2$, respectively. We found that the misalignment tolerance is much higher for both cases when using the AGC. For example, if the plasmonic waveguide center is at the edge of the silicon waveguide (i.e., $d_1$ = 150 nm) as shown in Fig. 3(a), the coupling efficiency is about 1% without using the AGC and about 26% when the AGC is used. In another example, if the MDM waveguide is placed next to the AGC (i.e., $d_2$ = 170 nm) as shown in Fig. 4(c), then coupling efficiency is negligible without using the AGC and about 41% when the AGC is used. Note that there is almost no alignment overlap between the dielectric waveguide and the MDM plasmonic waveguide. From this analysis, it is obvious that in order to achieve high coupling efficiency, the AGC's edges should be aligned to the silicon waveguide edges and the MDM waveguide should be placed at the center of the silicon waveguide.

#114470 - $15.00 USD Received 21 Jul 2009; revised 14 Sep 2009; accepted 22 Sep 2009; published 7 Oct 2009

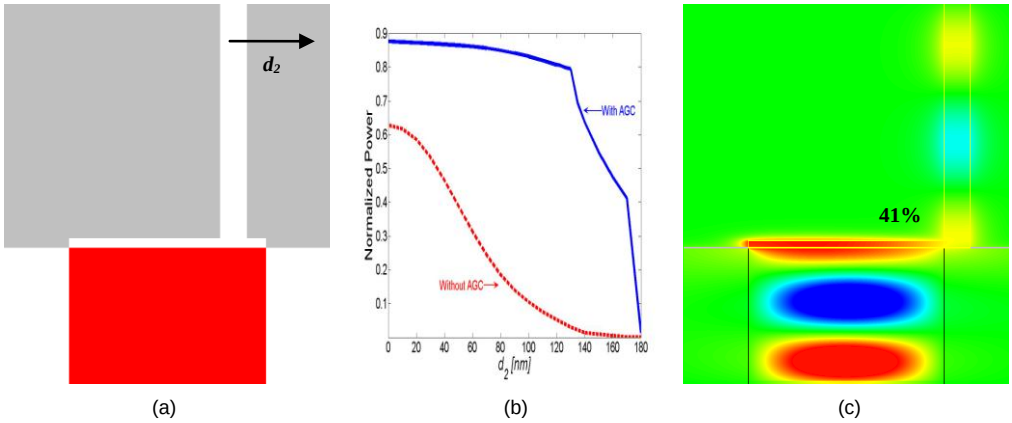


Fig. 4. (a) Schematic of the position misalignment $d_2$ between the silicon waveguide with the AGC connected to it and the plasmonic waveguide. (b) Coupling efficiency as a function of $d_2$. (c) Field distribution for the structure shown in Fig. 4(a) when $d_2$ = 170 nm.

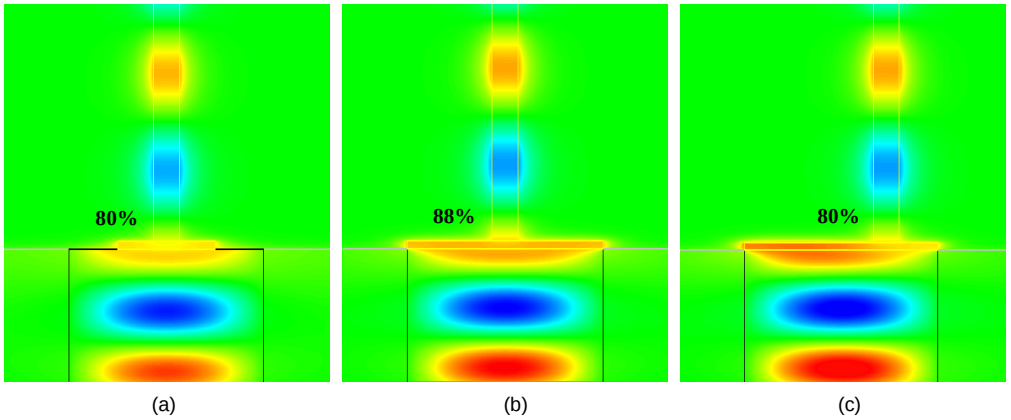


Fig. 5. The electric field distribution when (a) the width of the AGC does not match that of the silicon waveguide, (b) the width of the AGC matches that of the silicon waveguide and the MDM waveguide is at the center, and (c) the width of the AGC matches that of silicon waveguide and the MDM waveguide is not at the center.

In our couplers, the rectangular air-gap plays an important role in increasing both the coupling efficiency (as shown in Fig. 1) and improving the alignment tolerance of the plasmonic waveguide with respect to the dielectric waveguide (as shown in Figs. 3 and 4). To verify this, we made several additional simulations and found that without using the AGC the plasmonic mode was excited at the interface between metal and silicon that had a different mode size than that of the MDM waveguide. After using the AGC, the plasmonic mode size partially matched that of the MDM waveguide because the AGC formed a cavity between the metal and silicon, which enabled more power to couple into the MDM waveguide. When the AGC does not have the same width as that of the silicon waveguide, the SPP excitation starts from the area that is not covered with the AGC. Then the SPP is coupled inside the AGC and propagates towards the MDM waveguide and couples into the MDM waveguide, as shown in Fig. 5(a). When AGC covers the whole silicon area and the MDM waveguide is at the center, as shown in Fig. 5(b), the SPP excitation starts at an equal distance from the MDM waveguide and then is coupled into the MDM waveguide. When the MDM waveguide is not at the center, SPP excitation starts away from the MDM waveguide before it is coupled into the MDM waveguide [Fig. 5(c)]. This proves that the MDM waveguide introduces transverse

#114470 - $15.00 USD Received 21 Jul 2009; revised 14 Sep 2009; accepted 22 Sep 2009; published 7 Oct 2009

metal boundaries that prevent the transverse leakage of SPPs and consequently increases the coupling efficiency.

We can further explain why one structure has higher coupling efficiency than another. For example, the coupling efficiency for the structure shown in Fig. 1(c) has the highest coupling efficiency (about 88%) because the SPP excitation starts at equidistance from both sides of the centered MDM waveguide and are "funneled" into the MDM waveguide. In another example, the coupling efficiency for the structure shown in Fig. 5(a) is less than that for the structure shown in Fig. 1(c) because part of the excited SPP propagates away from the AGC and also the excited SPP mode at the interface between silicon and metal travels towards the AGC, which has a different dielectric material (air). On the other hand, when the width of the AGC is higher than that of the silicon waveguide, the AGC does not act as a cavity because the bottom of the extra length is terminated by air and not by silicon. Thus, the coupling efficiency dropped dramatically.

### 3. Splitter design

Ultra compact splitters are required in nanophotonic circuits in order to minimize the required area to produce multiple photonic devices on the same chip. The coupler introduced in the previous section can be easily used to design splitters. In this section, two methods were used to design splitters: one method by using the AGC and the other one without using the AGC.

In the first method, we designed a 3-dB splitter by increasing the separation distance $g_1$ between the two MDM waveguides [as shown in Fig. 6(a)] until maximum coupling is achieved. We found that the maximum coupling efficiency is about 37% for each branch when $g_1$ = 160 nm, as shown in Figs. 6(b) and 6(c). This configuration has the advantage in easy fabrication.

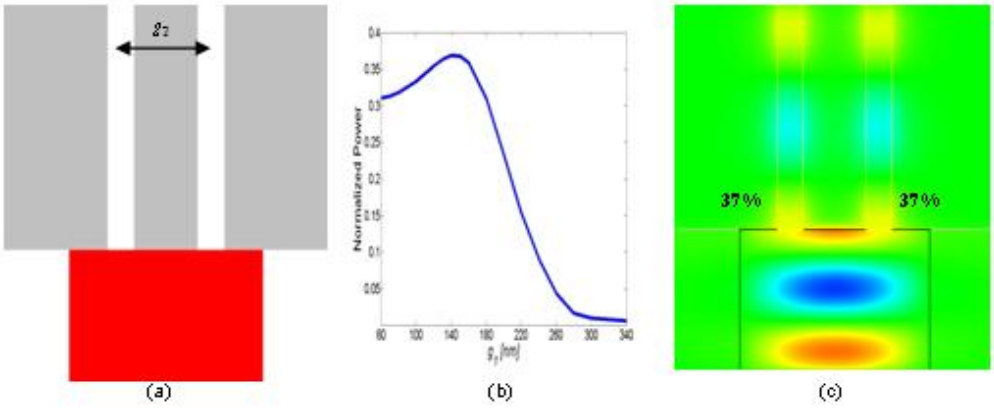


Fig. 6. (a) Schematic of the splitter structure without the air-gap coupler. (b) Coupling efficiency as a function of the separation distance $g_1$. (c) Field distribution for the structure shown in Fig. 6(a) for $g_1$ = 160 nm.

The efficiency can be further increased using the air-gap coupler. In the second method, we designed a 3-dB splitter by increasing the separation distance $g_2$ between the two MDM waveguides [as shown in Fig. 7(a)] until maximum coupling is achieved. The increase in $g_2$ was done after the addition of the rectangular AGC. We found that the maximum coupling efficiency is about 45% for each branch for $g_2$ = 260 nm, as shown in Figs. 7(b) and 7(c). Over 90% of power in total can be delivered into two MDM plasmonic waveguides.

#114470 - $15.00 USD Received 21 Jul 2009; revised 14 Sep 2009; accepted 22 Sep 2009; published 7 Oct 2009

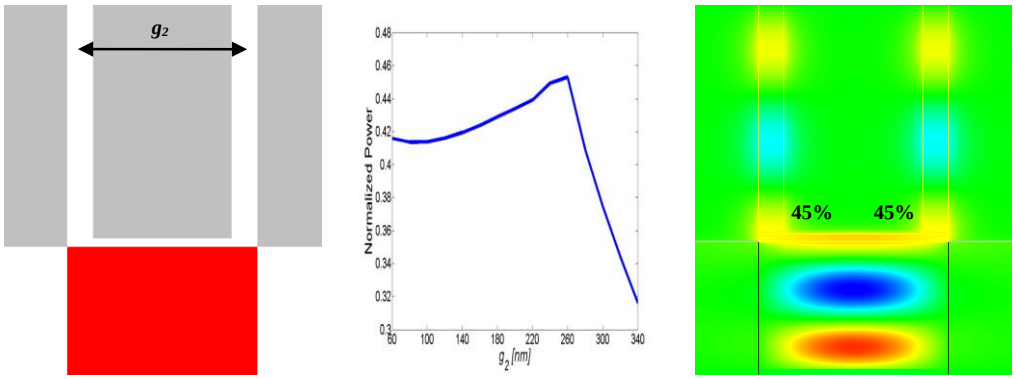


Fig. 7. (a) Schematic of the splitter structure with the air-gap coupler. (b) Coupling efficiency as a function of the separation distance $g_2$. (c) Field distribution for the structure shown in Fig. 7(a) for $g_2$ = 260 nm.

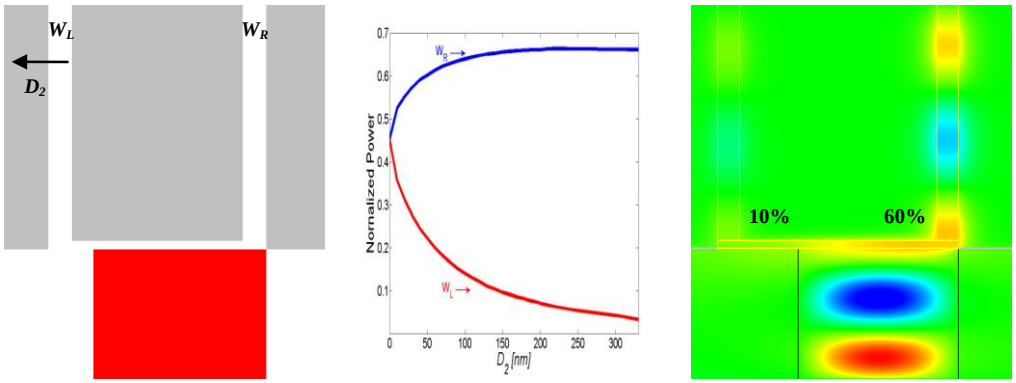


Fig. 8. (a) Schematic of the asymmetric splitter structure. (b) Coupling efficiency as a function of the displacement $D_2$. (c) Field distribution for $D_2$ = 150 nm.

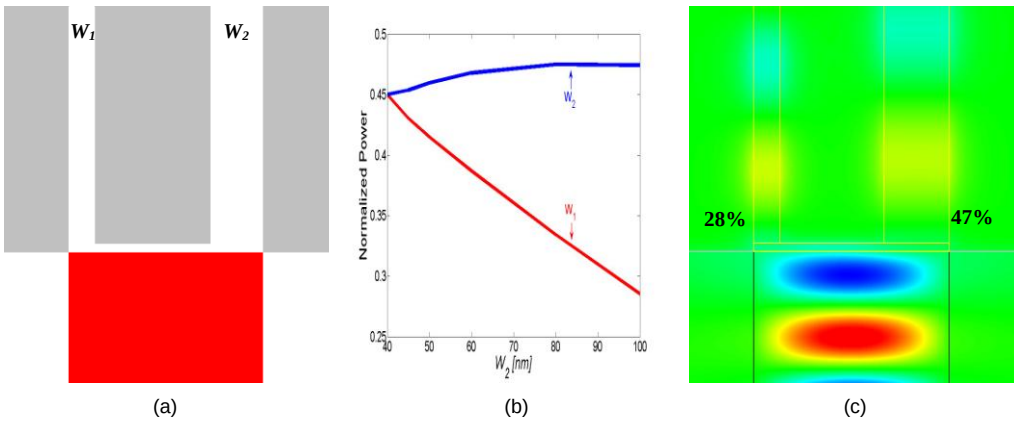


Fig. 9. (a) Schematic of the asymmetric splitter structure. (b) Coupling efficiency as a function of $W_2$. (c) Field distribution for $W_2$ = 100 nm and $W_1$ = 40 nm.

The splitting ratio can be easily controlled by the position of the MDM waveguides $W_R$ and $W_L$, as shown in Fig. 8(a). Before shifting $W_L$, the displacement between the two

#114470 - $15.00 USD Received 21 Jul 2009; revised 14 Sep 2009; accepted 22 Sep 2009; published 7 Oct 2009

waveguides was 260 nm, which resulted in a coupling efficiency of 45%. As expected, we found that as $D_2$ increases, coupling efficiency into the shifted waveguide decreases and coupling efficiency into the fixed waveguide increases [as shown in Fig. 8(b)]. Figure 8(c) shows the coupling efficiency ratio between $W_L$ and $W_R$ for $D_2$ = 150 nm. Even when there is no overlap between the shifted MDM waveguide and silicon waveguide, the coupled power is about 10% in $W_L$.

Another way to control the splitting ratio is by varying the width of MDM waveguides $W_1$ and $W_2$, as shown in Fig. 9(a). We found that as the width of $W_2$ increases from 40 nm to 100 nm, the coupling efficiency in $W_2$ increases slightly from 45% to 47%, while the coupling efficiency in a 40 nm wide $W_1$ decreases from 45% to 28% [as shown in Fig. 9(b)]. The field distribution for $W_2$ = 100 nm and $W_1$ = 40 nm is shown in Fig. 9(c).

## 4. Spectrum analysis

The proposed couplers and splitters can also operate at a broad frequency range. To show that, we varied the wavelength of the light source and measured the corresponding coupling efficiency. The coupling efficiency with respect to wavelength for the structures shown in Figs. 1(c) (with and without AGC), 5(c), and 6(c) is shown in Fig. 10(a). Using AGC broadens the spectrum range around the communication wavelength 1.55 μm for all structures. Using two plasmonic waveguides in addition to AGC broadens the spectrum over longer range. The wavelength dependent of the permittivity of metal is not very clear because the coupling efficiency is measured close to the interface with silicon. If the coupling efficiency is measured far away from the interface, then it will be obvious that the losses of the metal increase significantly as the wavelength decreases.

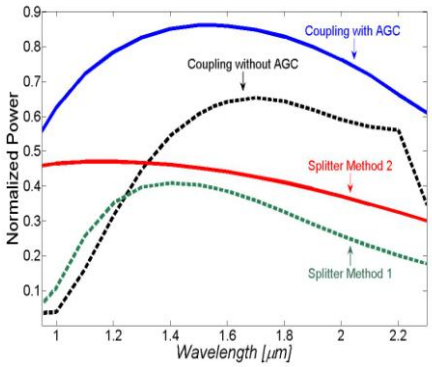


Fig. 10. Spectrum of the structures shown in Fig. 1(c) (with and without the AGC) and Figs. 5(c) and 6(c).

## 5. Conclusions

To summarize, we showed that a matching coupler at the interface between a dielectric waveguide and a plasmonic waveguide can be designed to increase the coupling efficiency as well as the alignment tolerance when aligning a dielectric waveguide to a plasmonic waveguide. In addition, based on the efficient couplers, nano-scale plasmonic 1 × 2 splitters can be designed with a coupling efficiency of 45% for each branch that operates at the optical telecom wavelength. The splitting ratio can be controlled by varying either the relative position or width of the two branches. Finally, we investigated the spectrum of the proposed structures and found that using the air-gap coupler broadens the spectrum around the optical communication wavelength. Two potential applications of our proposed coupler and splitter: a directional coupler and a Mach-Zehnder interferometer are presented in [17].

#114470 - $15.00 USD Received 21 Jul 2009; revised 14 Sep 2009; accepted 22 Sep 2009; published 7 Oct 2009